Simultaneous Time and Frequency Domain Solutions of EM Problems Using Finite Element and CFH Techniques

M. A. Kolbehdari, Meera Srinivasan, *Student Member, IEEE*, Michel S. Nakhla, *Senior Member, IEEE*, Qi-Jun Zhang, *Senior Member, IEEE*, and Ramachandra Achar, *Student Member, IEEE*

Abstract— **This paper describes an efficient method for both time- and frequency-domain solutions of electromagnetic (EM) field problems. In this method EM field problems are formulated using Laplace-domain finite element approach and are solved using complex frequency hopping (CFH) technique. CFH is a moment-matching technique which has been used successfully in the circuit simulation area for solution of large set of ordinary differential equations. Problems consisting of Dirichlet, Neumann and combined boundary conditions can be solved using the proposed algorithm to obtain both time and frequency responses. Several electromagnetic field problems have been studied using the new technique and the speed-up advantage (one to three orders of magnitude) compared to conventional finite element technique is demonstrated. A good agreement between numerical results obtained using the proposed method and the previously published results has been found.**

I. Introduction

MODELING and simulation based on electromagnetic field formulations are important for accurate analysis and design of high-speed circuits and systems [1], [2]. One of the most common approaches used for the solution of electromagnetic field problems is the finite element method (FEM) [3]–[7]. FEM formulations are either space/frequency-domain or space/time-domain. Space/frequency formulation leads to a set of algebraic equations which have to be solved repeatedly at many frequency points, while space/time formulation leads to a set of ordinary differential equations which have to be solved in the time-domain. The size of the equations to be solved is usually large and the conventional solution algorithms are restricted by computing time and stability condition. For example, frequently used time-stepping schemes [8]–[12] require the satisfaction of the stability condition, that is, the ratio of spatial to temporal subdivision is to be greater than or equal to the speed of propagation [13]. This means the finer the mesh, the smaller the time step that must be chosen [14]. Implicit variable time step integration algorithms [15] can be used. However, they require solution of large set of algebraic equations at each time point. Frequently, both time-domain and frequency-domain results are of interest [10]–[11]. In this case, fast fourier transform (FFT) and its inverse can be used to move from one solution space to the other. This can increase the computational time since in order to achieve satisfactory resolution, FFT has to span longer time and frequency intervals with smaller increments [16]. In an attempt to improve the efficiency of FEM solution techniques, a Laplace domain FEM has been proposed in [17]. This method is an extension of the technique used for solution of heat transfer problems [18]–[19]. However, it is based on congruence transformation which involves computationally expensive process of determining all the eigenvalues and eigenvectors of a large matrix.

From the conceptional point of view, the new technique proposed in this paper falls in the category of [17]–[19]. However, the main difference is that it requires the computation of the dominant natural modes only and thus eliminating the major computing cost.

The new solution technique is based on complex frequency hopping (CFH) [20]–[23], an expansion of asymptotic waveform evaluation (AWE) [24] recently developed in the circuit simulation area, which yields a speed-up factor of 10–1000 over conventional circuit simulators. It has been extended to solution of static fields in VLSI interconnects [25], in ground/power planes [26] and thermal equations [27]. CFH uses the concept of moment matching to obtain both frequency- and time-domain responses of large linear networks through a lower order multipoint Padé approximation. It extracts a relatively small set of dominant poles to represent a large network that may contain hundreds to thousands of actual poles. CFH is particularly suitable for solving large set of ordinary differential equations which make it a logical candidate for solving time-harmonic EM equations. The main steps involved can be summarized as follows: first, the given problem which is in the form of damped wave equation is formulated using FEM and the resulting ordinary differential equation is transformed to the Laplace domain; second, the Laplace domain output is expanded using Padé approximation at selected frequency points; third, information from each expansion point is used to generate the output frequency response or alternatively a unified set of dominant pole/residue pairs; finally, the results are transformed to the time-domain in either analytical or numerical form.

The main advantages of the proposed method can be summarized as follows:

Manuscript received June 29, 1995; revised May 24, 1996. This work was supported in part by the Natural Sciences and Engineering Research Council of Canada, Micronet, a Canadian Network of Centres of Excellence on Microelectronics Devices, Circuits and Systems, and Bell-Northern Research.

The authors are with the Department of Electronics, Carleton University, Ottawa, Ont, K1S 5B6 Canada.

Publisher Item Identifier S 0018-9480(96)06397-1.

1) 10–1000 times faster than the conventional FEM solution techniques;
2) solution algorithm does not suffer from instability problems associated with the time-stepping methods;
3) produces simultaneously both the time- and frequency-domain results.

The remaining part of this paper is organized as follows: in Section II, the damped wave equations are derived from Maxwell's equations and formulated using variational techniques. Section III describes the AWE and CFH techniques in the context of solving the FEM equations. To illustrate the accuracy and efficiency of the proposed method, Section IV presents numerical results for several electromagnetic field problems. The efficiency of the proposed method is illustrated and discussed in Section V. Finally a brief conclusion of the paper is presented in Section VI.

II. Formulation

For a homogeneous, isotropic, and a linear medium, starting from Maxwell's equations the following scalar equation can be derived as

$$\nabla^2\Phi - \epsilon\mu\frac{\partial^2\Phi}{\partial t^2} - \sigma\mu\frac{\partial\Phi}{\partial t} = f(x,y,z,t) \tag{1}$$

where $\Phi(x,y,z,t)$ represents either the electric or magnetic field components, and ϵ, μ, σ are the permittivity, permeability, conductivity of the medium respectively. $f(x,y,z,t)$ is related to the external excitation which could be function of time, space or both. This expression can be applied to either a diffusion problem where the second term in the left-hand-side of (1) is dropped or to a wave equation where the third term is dropped. Applying the finite element method [13] to (1) where the interpolating functions are selected in exactly the same fashion as compared to the time independent problems except now the nodal values are taken to be functions of time rather than constants. Expanding the unknown function Φ in the triangular finite element domain Ω_e as

$$\Phi(x,y,z,t) = \sum_{n=1}^{N_{e_p}} \Phi_i(t)\alpha_i(x,y,z) \tag{2}$$

where N_{e_p} is the total number of nodes in element Ω_{e_p}, $\Phi_i(t)$ denotes the local set of unknown time dependent expansion coefficients and $\alpha_i(x,y,z)$ are nodally based interpolation functions such as those regularly used in FEM triangular formulations [7]. It is of interest to note that in (2), the spatial variables x, y and z are discretized whereas the temporal variable t is not. An appropriate functional to be minimized for (1) is

$$F(\Phi) = \int_\Omega \left(\frac{1}{2}\mid\nabla\Phi\mid^2 + \epsilon\mu\Phi\Phi'' + \sigma\mu\Phi\Phi' + f\Phi\right)d\Omega \tag{3}$$

where Ω represents the finite element region. By minimizing the functional of the problem and applying associated Dirichlet and Neumann boundary conditions, a system of ordinary differential equations is obtained as

$$\mathbf{A}\Psi + \sigma\mu\hat{\mathbf{B}}\Psi' + \epsilon\mu\hat{\mathbf{C}}\Psi'' = \mathbf{q} \tag{4}$$

where Ψ, $\mathbf{A}$, $\hat{\mathbf{B}}$, $\hat{\mathbf{C}}$, and $\mathbf{q}$ are defined as follows

$$\Psi = \{\Phi_i\};\ i = 1,\ldots,N \tag{5}$$

$$\mathbf{A} = \sum_{e_p=1}^{N_e}[\mathbf{S}]_{e_p} \tag{6}$$

$$\hat{\mathbf{B}} = \hat{\mathbf{C}} = \sum_{e_p=1}^{N_e}[\mathbf{T}]_{e_p} \tag{7}$$

$$\mathbf{q} = \sum_{e_p=1}^{N_e}[\mathbf{G}]_{e_p} \tag{8}$$

where N_e denotes the total number of elements. $\mathbf{A}$, $\hat{\mathbf{B}}$, and $\hat{\mathbf{C}}$ are $N\times N$ symmetric, positive definite matrices assembled from $[\mathbf{S}]_{e_p}$ and $[\mathbf{T}]_{e_p}$ and N is the total number of nodes. $\mathbf{q}$ is a vector of dimension N, assembled from $[\mathbf{G}]_{e_p}$, containing the forced terms attributed to the time or space excitation. $[\mathbf{S}]_{e_p}$ and $[\mathbf{T}]_{e_p}$ are real symmetric square element matrices and $[\mathbf{G}]_{e_p}$ is a column vector given by

$$[\mathbf{S}_{ij}]_{e_p} = \int_{\Omega_{e_p}} \nabla\alpha_i^p\cdot\nabla\alpha_j^p\,d\Omega_{e_p} \tag{9}$$

$$[\mathbf{T}_{ij}]_{e_p} = \int_{\Omega_{e_p}} \alpha_i^p\alpha_j^p\,d\Omega_{e_p} \tag{10}$$

$$[\mathbf{G}_i]_{e_p} = \int_{\Omega_{e_p}} \alpha_i^p f(t)\,d\Omega_{e_p} \tag{11}$$

subject to the initial conditions

$$\Psi(0) = \Psi_0 \tag{12}$$

$$\Psi'(0) = \Psi_0' \tag{13}$$

where Ω_{e_p} denotes the domain of the finite elements. In (9) to (11) p refers to either 1, 2, or 3 corresponding to one, two, or three-dimensional (3-D) finite element solution scheme while α^p is the corresponding shape function and e_p represents the finite elements. Taking the Laplace transform of (4) results in

$$(\mathbf{C}s^2 + \mathbf{B}s + \mathbf{A})\mathbf{X}(s) = \mathbf{R}(s) \tag{14}$$

or

$$\mathbf{Y}(s)\mathbf{X}(s) = \mathbf{R}(s) \tag{15}$$

where $\mathbf{B} = \mu\sigma\hat{\mathbf{B}}$, $\mathbf{C} = \epsilon\mu\hat{\mathbf{C}}$, $\mathbf{X}(s) = \mathcal{L}[\Psi(t)]$, and $\mathbf{R}(s)$ is given by

$$\mathbf{R}(s) = s\mathbf{C}(\Psi_0 + \Psi_0') + \mathbf{B}\Psi_0 + \mathbf{Q}(s) \tag{16}$$

where $\mathbf{Q}(s) = \mathcal{L}[\mathbf{q}(t)]$.

III. Moment Matching Techniques

Moment matching techniques such as asymptotic waveform evaluation (AWE) [24] and complex frequency hopping (CFH) [21] have been topics of intense research in the circuit simulation area in the recent years. They have been successfully and efficiently applied for obtaining the solution of large set of ordinary differential equations.

In general, moment matching technique approximates the frequency response of a Taylor series expansion in the complex s-plane. The cost of an expansion is approximately one frequency point analysis. The moments (coefficients of the expansion) are matched to a lower order transfer function using a rational Padé approximation. This transfer function can be used to obtain the output response. The moments are generally taken from an $s = 0$ expansion (Maclaurin series). Single Padé approximations are accurate near the point of expansion in the complex s-plane and decrease in accuracy with increased distance from the point of expansion. Complex frequency hopping overcomes this problem and is summarized in the following section.

A. Complex Frequency Hopping

Complex frequency hopping is a method by which the frequency response of a system is expanded in multiple Taylor series expansions in the Laplace s-domain. The expansion points are chosen on or near the imaginary axis because poles that dominate the transient and frequency response of a system are found there. The moments of the expansion are then matched to a rational Padé approximation. These Padé approximations have several useful properties, one of which is the convergence of the poles of the approximation to the actual poles of a system. There are two approaches for generating the response of a system.

In the first approach [20], [21], several expansion points are generated and the converged poles from each expansion are compared. If two expansions have the same poles, then they are considered accurate within the radius of accuracy defined by those poles. If no poles are found in common, then an intermediate hop (expansion) is chosen. All poles within the radius of accuracy of each hop are then collected giving the actual system poles near the imaginary axis. The frequency and transient responses are then a closed-form function of these poles and their residues.

In the second approach [22], in order to obtain the frequency response, a set of rational transfer functions are generated at a minimized set of expansion points. It is the value of these transfer functions that is compared at points intermediate to the expansion points rather than a search for same poles. If two transfer functions are found to give the same frequency response at an intermediate frequency point between the two generating hops then these transfer functions are considered accurate. If this is not the case, then another hop is chosen between the two expansion points and an expansion is performed there. It was found empirically that this approach generally requires lesser number of hops compared to the first approach. This means that the CPU time can be reduced. Further reduction was also noted due to the fact that no pole convergence was required at each expansion point.

Summarizing, CFH ensures accuracy of an approximation for a complete frequency range, using multiple expansion points and corresponding Padé approximations at the frequencies of interest. Additional hops are generated at an incremental CPU cost above the cost of the first. However, the number of hops typically needed ranges from 2–15, far less than full FFT analysis requiring hundreds or thousands of frequency point analyzes.

B. Padé Approximation

Consider the response vector $\mathbf{X}(s)$ represented in (15). Taylor's series expansion of the output $\mathbf{X}(s)$ about a complex frequency point $s = s_o$, is given by

$$\mathbf{X}(s) = \sum_{n=0}^{\infty} \mathbf{M}_n (s - s_o)^n \tag{17}$$

where $\mathbf{M}_n$ is the nth moment vector of the Taylor's expansion about s_o and is given by

$$\mathbf{M}_n = \frac{\partial^n [\mathbf{Y}^{-1}(s)\mathbf{R}(s)]|_{s=s_o}}{\partial s^n} \Big/ n! \tag{18}$$

A recursive equation for the evaluation of the moments can be obtained in the form

$$[\mathbf{Y}(s_o)]\mathbf{M}_n = -\sum_{r=1}^{n} [\mathbf{Y}]^r \mathbf{M}_{n-r}/r! \tag{19}$$

where

$$[\mathbf{Y}]^r = \frac{\partial^r}{\partial s^r}\mathbf{Y}\Big|_{s=s_o}.$$

For each expansion point, the moments $m_n = [\mathbf{M}_n]_{(i)}$; $n = 0, 1, 2, \ldots (2q-1)$ of an output i are matched to a lower order frequency-domain function in the form

$$H(s) = X_{[i]}(s) = \frac{P_L(s)}{Q_M(s)} = \frac{\sum_{j=0}^{L} a_j s^j}{1 + \sum_{j=1}^{M} b_j s^j} \quad \text{for } 0 < s \le j\omega_n. \tag{20}$$

For given L and M, the coefficients of the numerator and denominator of the transfer function are related to the moments by

$$\begin{bmatrix} m_{L-M+1} & m_{L-M+2} & \cdots & m_L \\ m_{L-M+2} & m_{L-M+3} & \cdots & m_{L+1} \\ \vdots & \vdots & \vdots & \vdots \\ m_L & m_{L+1} & \cdots & m_{L+M-1} \end{bmatrix} \begin{bmatrix} b_M \\ b_{M-1} \\ \vdots \\ b_1 \end{bmatrix} = -\begin{bmatrix} m_{L+1} \\ m_{L+2} \\ \vdots \\ m_{L+M} \end{bmatrix} \tag{21}$$

$$a_r = \sum_{j=0}^{r} m_{r-j} b_j \tag{22}$$

where $r = 0, 1, \ldots, L$ and $m_j = 0$ if $j < 0$.

C. Binary Search Algorithm

Padé approximation is very accurate near the point of expansion i.e., $s = s_0$. However, the accuracy of Padé

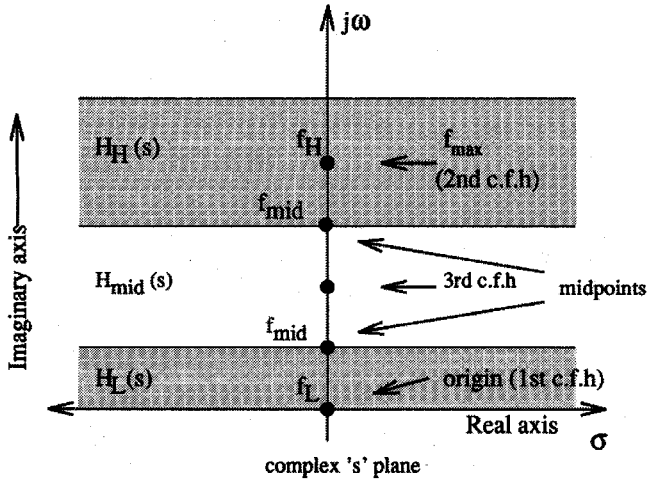

Fig. 1. Generation of transfer function by CFH.

approximation decreases as we move further away from the point of expansion similar to the case of a Taylor's series expansion.

In order to check the accuracy of an approximation, two expansion points are necessary. The accuracies of these two expansion points can be verified by matching the poles generated at these two expansion points [20], [21]. Alternatively, the two expansion points can be verified for their accuracy by finding the value of the transfer function at a point intermediate to these two expansion points [22]. Number of expansions required to obtain a fairly accurate set of transfer functions over a specified frequency range is controlled by a binary search algorithm.

The steps involved in the binary search algorithm for the second approach is summarized below.

Step 1) Set $f_L = 0$ and $f_H = f_{\max}$ (Fig. 1)

Step 2) Expand the system's response at frequency $f = f_L$. Determine the coefficients of the corresponding transfer function $H_L(s)$ using (21) and (22).

Step 3) Expand the system's response at frequency $f = f_H$. Determine the coefficients of the corresponding transfer function $H_H(s)$.

Step 4) Set $f = \frac{1}{2}(f_L + f_H)$. Calculate $H_L(j2\pi f)$ and $H_H(j2\pi f)$. If, $|H_H(j2\pi f) - H_L(j2\pi f)| < \epsilon$, where ϵ represents pre-specified threshold for relative error, GO TO Step 5. Otherwise expand at $f_{\text{mid}} = \frac{1}{2}(f_L + f_H)$ and determine $H_{\text{mid}}(s)$.

Step 5) If no middle frequency f_{mid} is generated between any two other frequency expansions, STOP, ELSE, repeat Steps 2–4 between every two consecutive frequency points (e.g., between f_L & f_{mid} and f_{mid} & f_H).

A similar search algorithm can be used for the first approach [21].

At the completion of the binary search algorithm, a set of transfer functions are generated. The frequency response at a particular frequency point is computed by choosing a transfer function valid for that region. This is repeated for all other frequency points and the system's frequency response is computed. The time-domain response is obtained as a closed form function of the generated poles and residues or alternatively by using inverse fast fourier transform (IFFT).

D. Moments Generation

To derive an expression for moments $\mathbf{M}_n$, we can rewrite (14) using (16) and (17) at any arbitrary complex frequency point $s = s_o$, and expanding the right hand side of (14) using Taylor's series, we get

$$\begin{aligned}&\left[(s-s_o)^2\mathbf{C} + (s-s_o)\mathbf{B} + \mathbf{A} + (s-s_o)2s_o\mathbf{C}\right.\\&\left. + \mathbf{B}s_o + \mathbf{C}s_o^2\right]\sum_{n=0}^{\infty}\mathbf{M}_n(s-s_o)^n\\&= \left[\mathbf{R}(s_0) + \frac{(s-s_o)}{1!}\mathbf{R}'(s_0) + \frac{(s-s_o)^2}{2!}\mathbf{R}''(s_0)\right.\\&\left. + \cdots + \frac{(s-s_0)^n}{n!}\mathbf{R}^n(s_0)\right] \qquad (23)\end{aligned}$$

where $\mathbf{R}(s_o) = \mathbf{B}\Psi_0 + \mathbf{Q}(s_0)$, $\mathbf{R}'(s_0) = \mathbf{C}(\Psi_0 + \Psi_0') + \mathbf{Q}'(s_0)$, $\mathbf{R}''(s_0) = \mathbf{Q}''(s_0)\cdots$ and $\mathbf{R}^n(s_0) = \mathbf{Q}^n(s_0)$.

Equating the coefficients of the powers of $(s - s_o)$ on both sides, we get

$$\left[\mathbf{C}s_o^2 + \mathbf{B}s_o + \mathbf{A}\right]\mathbf{M}_o = \mathbf{R}(s_o) \qquad (24)$$

$$\left[\mathbf{C}s_o^2 + \mathbf{B}s_o + \mathbf{A}\right]\mathbf{M}_1 = -[\mathbf{B} + 2s_o\mathbf{C}]\mathbf{M}_o + \mathbf{R}'(s_0). \qquad (25)$$

Generalizing we have

$$\begin{aligned}&\left[\mathbf{C}s_o^2 + \mathbf{B}s_o + \mathbf{A}\right]\mathbf{M}_n\\&\quad = -\mathbf{B}\mathbf{M}_{n-1} - \mathbf{C}[2s_o\mathbf{M}_{n-1} + \mathbf{M}_{n-2}] + \frac{\mathbf{R^n}(s_0)}{n!} \qquad (26)\end{aligned}$$

for $n \geq 2$.

IV. Numerical Results

Example 1: For purposes of comparison the first problem chosen is an example reported in [17]. Consider a one-dimensional (1-D) diffusion problem shown in Fig. 2. The problem consists of a magnetic slot with bottom and side walls made of magnetic material with infinite permeability. The time dependent magnetic field is illuminated on the top surface of the magnetic slot producing a time dependent current flowing through a metal-filled slot of infinite length. The excitation of the magnetic field $f(t)$ in (1) on the top surface of the magnetic slot is $f(t) = H(t) = e^{\alpha t} - e^{\beta t}$, which is an EMP type excitation with $\alpha = -4.0 \times 10^6$ and $\beta = -4.76 \times 10^8$. The other parameters are $d = 1.0 \times 10^{-4}$ (m), $\mu = 4\pi \times 10^{-7}$ (H/m) and $\sigma = 5.76 \times 10^5$ (S/m). The boundary condition of the problem is $H(t) = 0$ at $x = 0$. Fig. 3 shows the normalized time-domain magnetic field obtained by the proposed method at three different points ($x = \frac{d}{4}$, $x = \frac{d}{2}$, and $x = \frac{3d}{4}$). The results are compared with the response obtained by solving the ordinary differential equation (4) using conventional implicit numerical integration method [28]. A good agreement is observed between these two methods. These results are also in agreement with the analytical solution reported in [17].

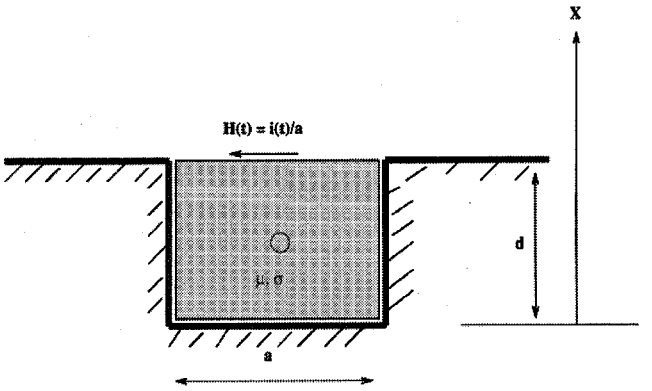

Fig. 2. The magnetic slot.

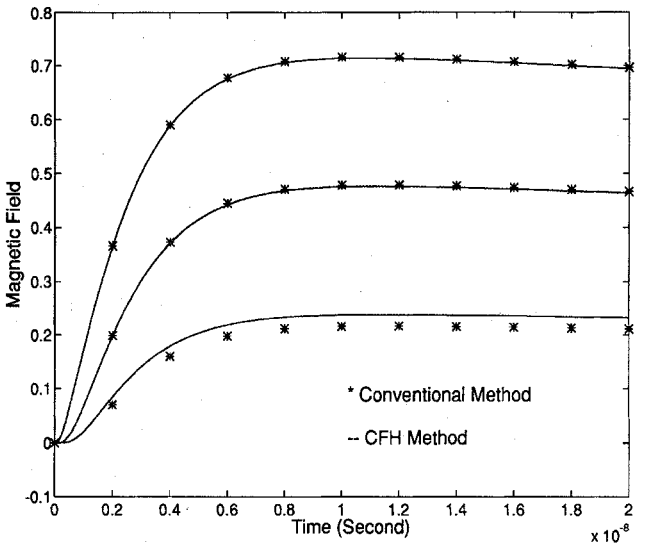

Fig. 3. Time-domain magnetic field distribution for the magnetic slot.

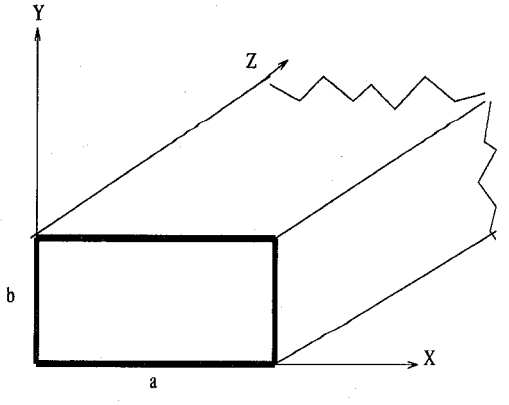

Fig. 4. The metallic rectangular waveguide.

Example 2: The second problem is a two-dimensional (2-D) metallic rectangular waveguide shown in Fig. 4. It is assumed that the waveguide is filled with a lossless dielectric material $\sigma = 0$ and its walls are perfectly conducting $\sigma_c = \infty$. For this problem it is also assumed that TM plane wave is propagated resulting in an electric field in the z-direction which can be determined from scalar wave equations. The other components of the field can be obtained from the

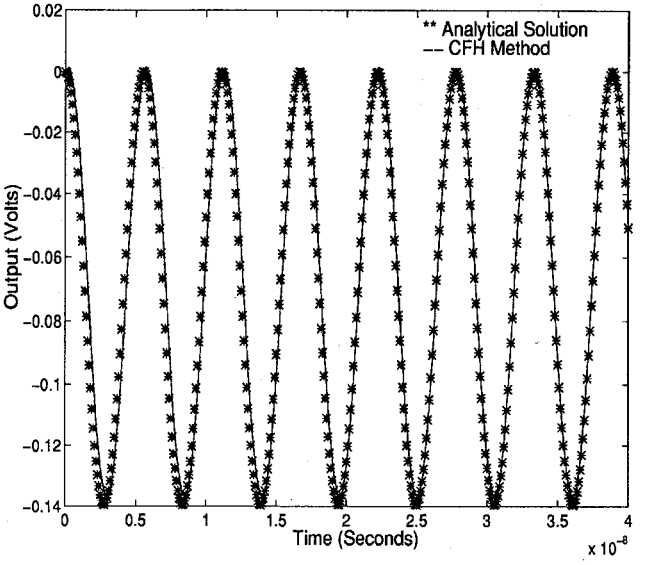

Fig. 5. Time-domain electric field distribution for the rectangular waveguide.

TABLE I
COMPARISON OF TRANSVERSE RESONANT FREQUENCIES OF THE RECTANGULAR WAVEGUIDE

Mode	FEM & CFH GHz	Analytical Solution $f = \frac{c}{2}\sqrt{(\frac{m^2}{a^2} + \frac{n^2}{b^2})}$ GHz
TM_{11}	.18102	.180152
TM_{21}	.25158	.249827
TM_{31}	.33749	.335178
TM_{13}	.46328	.460658
TM_{23}	.49702	.492102
TM_{51}	.52770	.521654
TM_{33}	.54890	.540458
TM_{61}	.62588	.618038
TM_{53}	.68161	.672215
TM_{63}	.73713	.749481

z-components of the electric field. The application of the proposed method is demonstrated for a rectangular waveguide with dimensions ($a = 1.5$ m and $b = 1.0$ m) subject to the boundary conditions

$$\Phi(x,1,t) = 0, \quad \Phi(x,0,t) = 0, \tag{27a}$$

$$\Phi(0,y,t) = 0, \quad \Phi(1.5,y,t) = 0 \tag{27b}$$

and the initial conditions are given by

$$\Phi(x,y,0) = 0, \quad \frac{\partial \Phi}{\partial t}(x,y,0) = 0 \tag{28}$$

where the right-hand side of the wave equation (1) is a function of space only given by

$$f(x,y) = \sin\left(\frac{2\pi x}{3}\right)\sin(\pi y) \tag{29}$$

on the domain of solution.

The problem reduces to that of a wave equation given by

$$\nabla^2 \Phi - \frac{1}{c^2}\frac{\partial^2 \Phi}{\partial t^2} = f(x,y) \tag{30}$$

TABLE II
CPU TIME COMPARISON

Matrix Size	FEM & CFH (seconds)	FEMFD (seconds)	Speed-up Ratio	Number of hops
25 × 25	.3	5.8	19	2
255 × 255	11.75	532.35	45	15
289 × 289	18.66	753.26	41	19
357 × 357	32.6	921.39	29	21
925 × 925	212.8	9364.68	45	23
1431 × 1431	500.33 (8.3 minutes)	36538.36 (10.1 hours)	72	14

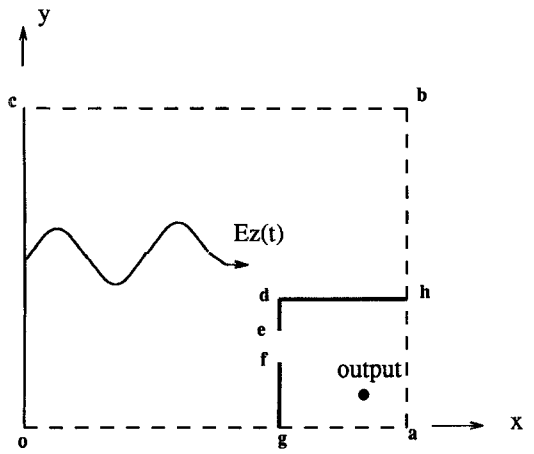

Fig. 6. Electromagnetic shield.

TABLE III
COMPARISON OF TRANSVERSE RESONANT FREQUENCIES (MHz) FOR AN ELECTROMAGNECTIC SHIELD

LDFEM	FEMFD	FEM & CFH
531.90	530.16	529.98
894.50	814.57	879.78
1132.00	1131.30	1131.15

The analytical solution of (30) can be obtained using the method of separation of variables given by

$$\Phi(x,y,t) = \frac{9}{13\pi^2}(\cos\omega t - 1)f(x,y) \tag{31}$$

where $\omega = \frac{\sqrt{13}\pi c}{3}$. Fig. 5 shows both the time-domain response of the electric field at ($x = \frac{3a}{4}$ and $y = \frac{b}{2}$) and the analytical solution (31). It is observed that the two responses are indistinguishable.

Example 3: Transverse resonance frequencies of the rectangular waveguide shown in Fig. 4 with the same dimensions are calculated by the proposed method where the excitation is at ($x = \frac{a}{4}$ and $y = \frac{b}{2}$) and output at ($x = \frac{3a}{4}$ and $y = \frac{b}{2}$). To verify the proposed method the transverse resonant frequencies of the rectangular waveguide are also calculated by the analytical solution and the results are compared in Table I. A good agreement between the results is observed. To illustrate the efficiency of the CFH technique, the transverse resonance frequencies were also calculated using the FEMFD approach where the frequency-domain response was obtained directly solving (14). CPU time comparison is shown in Table II.

TABLE IV
CPU TIME COMPARISON FOR THE ELECTROMAGNETIC SHIELD

FEMFD (sec)	FEM & CFH (sec)	Speed-up Ratio
17228.53	118.92	145

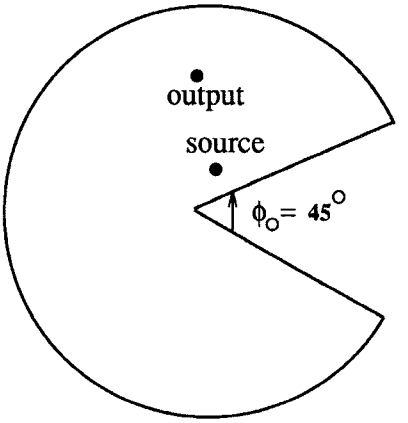

Fig. 7. Cylindrical waveguide.

Example 4: The example chosen here is an application to a 2-D shielding problem reported in [17]. The third term in (1) is dropped due to the omission of the conduction current and this corresponds to wave equations. The problem consists of two TM plane waves, independent of z-coordinate, oppositely impinge on a rectangular metallic cylinder serving as an electromagnetic shield, in which four slots or apertures are symmetrically located as shown in Fig. 6. The boundary conditions are as follows: $\frac{\partial \mathbf{E}_z(t)}{\partial y} = 0$ on cb and oa, $\frac{\partial \mathbf{E}_z(t)}{\partial x} = 0$ on ba.

A pulse is used as an excitation on the boundary co. The physical structure and the dimensions of the problem are as follows: the 2-D shield with slots is made of perfect conductor; the excitation source has no spatial variation in the z direction; $oa = 1.0$ m, $ga = 0.2$ m, $ha = 0.2$ m, $ba = 1.0$ m, $de = 0.05$ m and the slot width $ef = 0.05$ m. The location of the output is at $x = 0.9571$ m and $y = 0.05$ m. In [17], LDFEM is used to find the frequency response of the problem. Here, 841 nodes and 1568 elements were used in the FEM formulation. Transverse resonant frequencies are compared in Table III and CPU time comparison is shown in Table IV.

Example 5:

The problem chosen here is a cylindrical structure, problem 5.25 in [29]. The problem consists of a circular cavity with a conducting wedge as shown in Fig. 7. For a structure where

TABLE V
COMPARISON OF TRANSVERSE RESONANT FREQUENCIES (MHZ) FOR A CYLINDRICAL WEDGE WAVEGUIDE

Analytical Method	FEMFD	FEM & CFH
$TM_{01} = 154.50$	156.85	156.25
$TM_{11} = 245.65$	229.34	229.49
$TM_{21} = 329.08$	312.94	313.48
$TM_{02} = 353.80$	351.68	351.56

TABLE VI
CPU TIME COMPARISON FOR A CYLINDRICAL WEDGE WAVEGUIDE

FEMFD (sec)	FEM & CFH (sec)	Speed-up Ratio
3326.82	11.38	292

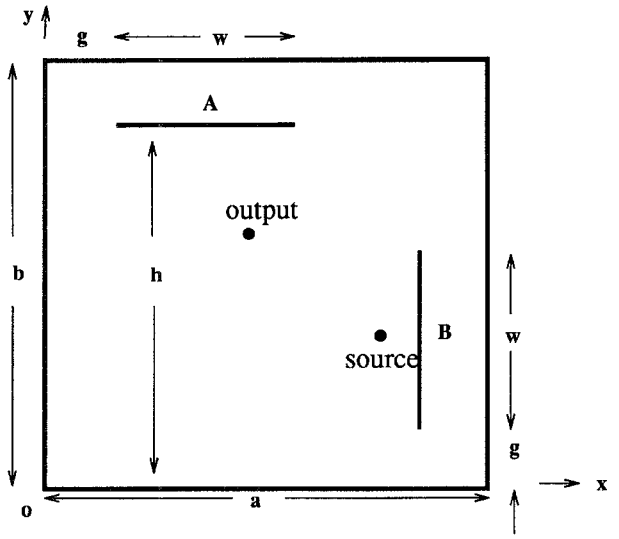

Fig. 8. Triple TEM cell.

the thickness is relatively much smaller than the radius of the waveguide a, the transverse resonant frequency of the dominant mode is given by

$$f_r = \frac{w}{2\pi a\sqrt{\epsilon\mu}} \tag{32}$$

where w is the first root of Bessel's function $J_v(w) = 0$ and $v = \frac{\pi}{(2\pi - \Phi_0)}$. For a specific case, w and f_r are calculated to be 3.28 and 154.5 MHz (32) where $\Phi_0 = 45°$, $v = 0.5714$, $a = 1.0$ m. For several modes the resonant frequency, f_r is calculated and is given in column one of Table V.

In this example, 396 nodes and 700 elements were used in the FEM formulation. The analytical results are compared with the results from FEMFD and FEM & CFH in Table V and CPU time comparison is shown in Table VI.

Example 6: The Triple-TEM or TTEM considered is an example reported in [30]. The TTEM cell has a tapered structure and has an additional electric field polarization in the transverse plane compared to conventional TEM cells. It also has two separately perpendicular inner conductors (septums) distinguishing it from GTEM cell. In [30], LDFEM is used to find the frequency response of TTEM cell. The cross sectional area of the TTEM cell is shown in Fig. 8. The problem domain

TABLE VII
COMPARISON OF TRANSVERSE RESONANT FREQUENCIES (MHZ) FOR A TTEM CELL

LDFEM	FEMFD	FEM & CFH
242.52	241.61	241.82
381.21	382.40	382.47
388.89	383.35	383.15
484.72	481.61	481.59
545.28	535.84	535.94
555.00	547.65	547.39
606.04	609.39	609.59
640.66	615.83	615.75

TABLE VIII
CPU TIME COMPARISON FOR A TTEM CELL

FEMFD (sec)	FEM & CFH (sec)	Speed-up Ratio
18393.43	25.92	710

is bounded by the following Dirichlet boundary conditions: septum A is set to 1 V while septum B is set to 0 V. The outer conductor is set to 0 V. The assumed excitation is a line source of $\mathbf{E}_z$ field for the TM modes. It is also assumed that the fields have no variations along the z-coordinate. The physical dimensions of the cell are: $a = 1.0$ m, $b = 1.0$ m, $w = 0.5$ m, $h = 0.875$ m and $g = 0.1875$ m. The number of degrees of freedom chosen in the finite element calculation was 676. The transverse resonant frequencies using the three different approaches are shown in Table VII. Table VIII shows a very good speed-up ratio for this problem.

V. DISCUSSION AND CPU ANALYSIS

The main reason behind the efficiency of the proposed approach is that it requires one LU decomposition per frequency hop, whereas FDFEM requires one LU decomposition at each frequency point. Generally, the number of frequency hops required is far less than the number of frequency points to get an accurate solution. To illustrate this, consider the CPU cost for the two approaches

$$(\mathrm{CPU})_{\mathrm{FDFEM}} = (\mathrm{CPU})_s + N_p \times [(\mathrm{CPU})_{\mathrm{LU}} + (\mathrm{CPU})_{\mathrm{FB}}] \tag{33}$$

$$(\mathrm{CPU})_{\mathrm{CFH}} = (\mathrm{CPU})_s + N_h \times [(\mathrm{CPU})_{\mathrm{LU}} + N_m \times (\mathrm{CPU})_{\mathrm{FB}}] \tag{34}$$

where $(\mathrm{CPU})_{\mathrm{FDFEM}}$ is the total cost for the FDFEM approach, $(\mathrm{CPU})_{\mathrm{CFH}}$ is the total cost for the FEM & CFH approach, $(\mathrm{CPU})_s$ is the time for reordering the sparse matrix, N_p is the number of frequency points considered, N_h is the total number of hops and N_m is the total number of moments. Table IX indicates the actual and expected speed-up ratio obtained for different examples included in this paper. The deviation from the expected value is due to the other factors being neglected in (33) and (34).

For sparse matrices, $(\mathrm{CPU})_{\mathrm{LU}}$ is proportional to N^α where N is the size of the matrix resulting from FEM formulation and α is problem dependent and ranges between 1.1 to 1.7 [15]. Assuming $(\mathrm{CPU})_{\mathrm{LU}}$ is the most dominant factor compared to

TABLE IX
COMPARISON OF SPEED-UP RATIO FOR DIFFERENT EXAMPLES

Experiments	Expected Speed-up N_p/N_h	Actual Speed-up $(CPU)_{FDFEM}/(CPU)_{CFH}$
Eg. 3, matrix size = 925	45	45
Eg. 3, matrix size = 1431	74	72
Eg. 4, matrix size = 841	164	145
Eg. 5, matrix size = 396	456	292
Eg. 6, matrix size = 676	820	710

the other CPU costs, we get *speed-up ratio* $\approx \frac{N_p}{N_h}$ and the CPU cost for the proposed FEM and CFH approach is

$$(\mathrm{CPU})_{\mathrm{CFH}} \simeq K N_h N^{\alpha} \tag{35}$$

where K is a constant.

VI. CONCLUSION

A new and efficient technique for simultaneously obtaining frequency- and time-domain response for electromagnetic field problems has been presented in this paper. The method is based on the Laplace domain finite element formulation and complex frequency hopping techniques. Several electromagnetic problems have been studied using the new method and an accurate match with the analytical solution has been found. A speed-up of one to three orders of magnitude compared to the conventional FEM technique has been obtained.

REFERENCES

[1] M. Nakhla and Q. J. Zhang, Eds., *Modeling and Simulation of High Speed VLSI Interconnects*. Boston, MA: Kluwer, 1995.

[2] Y. S. Tsuei, A. C. Cangellaris, and J. P. Prince, "Rigorous electromagnetic modeling of chip-to-package (first-level) interconnections," *IEEE Trans. Comp., Hybrids, Manufact. Tech.*, vol. 36, pp. 1775–1787, Dec. 1988.

[3] U. Ghoshai and L. N. Smith, "Finite element analysis of skin effect in copper interconnects at 77 K and 300 K," in *IEEE MTT-S Int. Symp. Dig.*, 1988, pp. 773–776.

[4] C. K. Tzuang and T. Itoh, "Finite element analysis of slow wave Schottky contact printed lines," *IEEE Trans. Microwave Theory Tech.*, vol. MTT-34, no. 2, pp. 1483–1489, 1986.

[5] M. A. Kolbehdari, "Analysis of quasistatic characteristic of cylindrical coupled micro-strip transmission line by finite element method," in *IEEE AP-MTT Benjamin Franklin Symp. Dig.*, May 1994, pp. 69–73.

[6] M. A. Kolbehdari and M. Sadiku, "Finite and infinite analysis of coupled cylindrical microstrip line in a nonhomogeneous dielectric media," in *Proc. IEEE Southeast Conf.*, Mar. 1995, pp. 269–273.

[7] P. P. Silvester and R. L. Ferrari, *Finite Elements for Electrical Engineers*. New York: Cambridge Univ. Press, 1990.

[8] J. Joseph, T. J. Sober, and K. J. Gohn, "Time domain analysis by the point-matched finite element method," *IEEE Trans. Magn.*, vol. 27, pp. 3852–3855, 1991.

[9] N. K. Madsen and R. W. Ziokowski, "Numerical solution of Maxwell's equations in the time domain using irregular nonorthogonal grids," *Wave Motion*, vol. 10, pp. 583–596, 1988.

[10] G. Mur, "The finite element modeling of three–dimensional electromagnetic fields using edge and nodal elements," *IEEE Trans. Antennas Propagat.*, vol. 41, no. 7, pp. 948–953, July 1993.

[11] S. Celozzi and M. Feliziani, "Time domain finite element simulation of conductive regions," *IEEE Trans. Magn.*, vol. MAG-29, pp. 1705–1710, 1993.

[12] P. J. Leonard and D. Rodger, "Some aspects of two and three dimensional transient eddy current modeling using finite element and single step time matching algorithms," *IEE Proc. Part-H*, 1988, vol. 135, pp. 159–166.

[13] D. S. Burnett, *Finite Element Analysis*. Reading MA: Addison-Wesley, 1988.

[14] I. A. Tsukerman, A. Konrad, G. Bedrosian, and M. V. K. Chari, "A survey of numerical methods for transient eddy current problems," *IEEE Trans. Magn.*, vol. 29, pp. 1711–1716, 1993.

[15] J. Vlach and K. Singhal, *Computer Methods for Circuit Analysis and Design*. New York: Van Nostrand, 1983.

[16] H. J. Nussbaumer, *Fast Fourier Transform and Convolution Algorithms*. New York: Springer-Verlag, 1982.

[17] X. D. Cai and G. I. Costache, "A Laplace domain finite element method (LDFEM) applied to diffusion and propagation problems in electrical engineering," *Int. J. Numerical Modeling, Electronic Networks, Devices and Fields*, vol. 7, pp. 419–432, 1994.

[18] H. T. Chen and C. K. Chen, "Hybrid Laplace transform/finite element method for two dimensional transient heat conduction," *J. Thermophysics*, vol. 2, pp. 31–36, 1988.

[19] C. K. Chen and T. M. Chen, "New hybrid Laplace transform/finite element method for three dimensional transient heat conduction problem," *Int. J. Num. Meth. Eng.*, vol. 32, pp. 45–61, 1991.

[20] E. Chiprout and M. Nakhla, *Asymptotic Waveform Evaluation and Moment Matching for Interconnect Analysis*. Boston: Kluwer, 1994.

[21] E. Chiprout and M. Nakhla, "Analysis of interconnect networks using complex frequency hopping," *IEEE Trans. Computer-Aided Design*, vol. 14, pp. 186–200, Jan. 1995.

[22] R. Sanaie, E. Chiprout, M. Nakhla, and Q. J. Zhang, "A fast method for frequency and time domain simulation of high speed VLSI interconnects," *IEEE Trans. Microwave Theory Tech.*, vol. 42, pp. 2562–2571, 1994.

[23] M. A. Kolbehdari, M. S. Nakhla, and Q. J. Zhang, "Solution of EM problems using finite element method and complex frequency hopping techniques," in *25th European Microwave Conf.*, Sept. 1995, vol. 2, pp. 1079–1081.

[24] L. T. Pillage and R. A. Rohrer, "Asymptotic waveform evaluation for timing analysis," *IEEE Trans. Computer-Aided Design*, vol. 9, pp. 352–366, 1990.

[25] S. Kumashiro, R. Rohrer, and A. Strojwas, "Asymptotic waveform evaluation for transient analysis of 3-D interconnect structures," *IEEE Trans. Computer-Aided Design*, vol. 12, pp. 988–996, 1993.

[26] E. Chiprout, M. Heeb, M. Nakhla, and A. E. Ruehli, "Simulating 3-D retarded interconnect models using complex frequency hopping," in *Proc. IEEE-ACM Int. Conf. Computer-Aided Design*, 1993, pp. 66–72.

[27] D. G. Liu, V. Phanilatha, Q. J. Zhang, and M. Nakhla, "Asymptotic thermal analysis of electronic packages and printed circuit boards," *IEEE Trans. Comp., Packag. Manuf. Technol.*, Part A, vol. 18, pp. 781–787, 1995.

[28] MATLAB *User's Guide*. Natick, MA: The Math Works, Inc., 1992.

[29] R. Harrington, *Time-Harmonic Electromagnetic Fields*. New York: McGraw-Hill, 1961.

[30] X. D. Cai and G. I. Costache, "Finite element analysis of a triple-TEM cell," *IEEE Trans. Electromagn. Compat.*, vol. 36, no. 4, pp. 398–404, Nov. 1994.

M. A. Kolbehdari received the B.S., M.S., and Ph.D. degrees in electrical engineering from the University of Communication, Tehran, Iran, the University of Mississippi, and Temple University, Philadelphia, PA, in 1984, 1989, and 1993, respectively.

He joined the Department of Electrical Engineering at Temple University as a Research Fellow in August 1993. Since October 1994, he has been with the Department of Electronics at Carleton University as a Research Associate Engineer. His research interests include applied electromagnetic, modeling and simulation of high frequency circuits, packaging, multichip modules, and high-speed VLSI interconnects, scattering and antennas.

Meera Srinivasan (S'96) received the B.Eng. degree in electrical engineering from Bangalore University, Bangalore, India in 1992.

Her professional experience in the field of power electronics in 1993 and 1994 mainly involved design and development of dc-dc converters and switch mode power supplies. She handled several independent projects at Electrohms Private Ltd., Bangalore, India. Presently she is pursuing the M.Eng. degree in the Department of Electronics at Carleton University, Ottawa, Canada. Her current research involves development of computer-aided design tools for design of high speed circuits and interconnects.

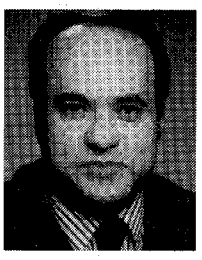

Michel S. Nakhla (S'73–M'76–SM'88) received the B.Sc. degree in electronics and communications from Cairo University, Egypt in 1967 and the M.A.Sc. and Ph.D. degrees in electrical engineering from Waterloo University, Ontario, Canada in 1973 and 1975, respectively.

In 1975, he was a Postdoctoral Fellow at University of Toronto, Ontario, Canada. In 1976 he joined Bell-Northern Research, Ottawa, Canada, as a Member of the Scientific Staff where he became Manager of the simulation group in 1980 and Senior Manager of the computer-aided engineering group in 1983. In 1988, he joined Carleton University, Ottawa, Canada, where he is currently a Professor in the Department of Electronics. His research interests include computer-aided design of VLSI and communication systems, high-frequency interconnects and synthesis of analog circuits. He is coauthor of *Asymptotic Waveform Evaluation* (Kluwer, 1994) and coeditor of *Modeling and Simulation of High-Speed VLSI Interconnects* (Kluwer, 1994).

Dr. Nakhla is the holder of the Computer-Aided Engineering Senior Industrial Chair established at Carleton University by Bell Northern Research and the Natural Sciences and Engineering Research Council of Canada.

Qi-Jun Zhang (S'84–M'87–SM'95) received the B.Eng. degree from the East China Engineering Institute, Nanjing, China in 1982, and the Ph.D. degree from McMaster University, Hamilton, Canada, in 1987, both in electrical engineering.

He was with the Institute of Systems Engineering, Tianjin University, Tianjin, China, from 1982 to 1983. He was a Research Engineer with Optimization Systems Associates Inc., Dundas, Ontario, Canada from 1988 to 1990. During 1989 and 1990 he was also an Assistant Professor of Electrical and Computer Engineering in McMaster University. He joined the Department of Electronics, Carleton University, Ottawa, Canada in 1990 where he is presently an Associate Professor. His professional interests include all aspects of circuit CAD with emphasis on large scale simulation and optimization, statistical design and modeling, neural networks, sensitivity analysis, and optimization of microwave circuits and high-speed VLSI interconnections. He is a coeditor of *Modeling and Simulation of High-Speed VLSI-Interconnects* (Kluwer, 1994) and a contributor to *Analog Methods for Computer-Aided Analysis and Diagnosis* (Marcel Dekker, 1988).

Dr. Zhang is the holder of the Junior Industrial Chair in CAE established at Carleton University by Bell-Northern Research and the Natural Sciences and Engineering Research Council of Canada.

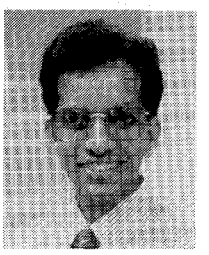

Ramachandra Achar (S'95) received the B.Eng. degree in electronics engineering from Bangalore University, India, in 1990, and the M.Eng. degree in micro-electronics from Birla Institute of Technology and Science, India, in 1992. Currently he is working toward the Ph.D. degree at Carleton University.

He spent the summer of 1995 working with the electrical modeling and simulation group at T. J. Watson Research Center, IBM, NY. He was a Graduate Trainee at Central Electronics Engineering Research Institute, Pilani, India in 1992. He was also previously employed at Larsen and Toubro Engineers Ltd., Mysore, India as a R&D Engineer at their ASIC design center and at Indian Institute of Science, Bangalore, India as a research assistant. His research interests include computer-aided design of high-speed systems and numerical algorithms.